Biophysical Characterization of Insoluble Aggregates of a Multi-Domain Protein: An Insight into the Role of the Various Domains

PIERRE O. SOUILLAC

Pharmaceutical Sciences and Technology group, Biogen Idec, 14 Cambridge Center, Cambridge, Massachusetts 02142

Received 13 February 2005; revised 9 May 2005; accepted 20 May 2005

Published online in Wiley InterScience (www.interscience.wiley.com). DOI 10.1002/jps.20423

ABSTRACT: Insoluble (visible) aggregates of a homodimer fusion glycoprotein, consisting of the first extracellular domain of a human protein, fused to the hinge, C_H2, and C_H3 domains of a human immunoglobulin G_1 (IgG_1), were observed during early formulation development. The soluble fraction of the fusion protein was compared to the visible aggregates by various biophysical techniques such as intrinsic and ANS fluorescence emission, reducing and nonreducing SDS–PAGE, equilibrium folding and refolding experiments in urea and guanidine hydrochloride in the absence and presence of mercaptoethanol. Significant differences were observed between the visible aggregates and the supernatant. Partial unfolding of the aggregated molecules was detected by intrinsic and ANS fluorescence. Using urea and guanidine hydrochloride unfolding/solubilization and refolding curves, it was possible to extrapolate that (i) the aggregates were not covalently linked but tightly associated, (ii) the fused domains of the protein were unfolded but not involved in the aggregation process, (iii) the C_H2 domains were native-like, and (iv) the C_H3 domains were involved in the aggregation process. © 2005 Wiley-Liss, Inc. and the American Pharmacists Association J Pharm Sci 94:2069–2083, 2005

Keywords: insoluble aggregates; protein; immunoglobin; mercaptoethanol

INTRODUCTION

Protein aggregation is not only the source of numerous human diseases,[1–4] but also a critical problem during the expression, purification, and storage of therapeutic proteins.[5,6,7] It has been hypothesized that protein aggregation occurs stepwise, a slow phase of nuclei formation (soluble oligomers) preceding a relatively fast growth phase, resulting in the formation of insoluble aggregates,[8,9] either as unordered (amorphous aggregates) or ordered (fibrils) structures. Nucleus formation has been hypothesized to originate from partially unfolded intermediates, transient species highly prone to aggregate. Thus, any factors influencing the formation of such aggregation-prone species will significantly impact the rate and extent of the aggregation process. It has been shown that submitting the same protein to slightly different destabilizing environments will result in different types of aggregates, depending on the conformation of the partially unfolded species.[10] Therefore, gaining basic information on the physical behavior and chemical degradation pathways[11,12] of proteins under various conditions is a key step of therapeutic protein formulation development. Despite considerable efforts to prevent it, protein aggregation is often encountered during formulation development of therapeutic proteins. Efficient solutions of such aggregation issues require an understanding of the cause and mechanism of aggregation, as well as characterization of the aggregated material.

Correspondence to: Pierre O. Souillac (Telephone: 617-914-4565; Fax 617-679-3416;
E-mail: pierre.souillac@biogenidec.com)

Journal of Pharmaceutical Sciences, Vol. 94, 2069–2083 (2005)
© 2005 Wiley-Liss, Inc. and the American Pharmacists Association

Regeneron Ex. 2073
Alvotech v. Regeneron
PGR2025-00085
Page 1 of 15
RGN-EYLEA-BIOSIM-00741165

Although mechanisms, causes, and kinetics of aggregation have been extensively studied,[13–17] limited attention has been focused upon characterization of visible aggregates as means of identifying regions of the protein molecule involved in the aggregation process.[18] Therapeutic proteins of large size (i.e., multi-domain proteins), with complex tertiary and quaternary structures, are becoming the norm, rendering extra difficulty to any investigation. Furthermore, the study of insoluble aggregates is limited by the number of applicable techniques, as the vast majority of biophysical techniques is only applicable to soluble material.

This study, which uses a relatively generic approach, illustrates the complementary use of several biophysical techniques[19] to characterize visible aggregates of a human multi-domain protein that were encountered during formulation development. Techniques such as intrinsic and ANS fluorescence emission, reducing and nonreducing SDS-PAGE, equilibrium unfolding/solubilization and refolding experiments in urea and guanidine hydrochloride in the absence and presence of 2-mercaptoethanol were used to deconvolute the involvement of each domain in the stabilization of particulates, despite the structural complexity of the protein.

EXPERIMENTAL

Chemicals

Urea, purchased from Spectrum (Gardena, CA), 2-mercaptoethanol from Fluka (Buchs, Switzerland), and all other chemicals, purchased from Sigma (St. Louis, MO), were of the highest grade available. The water used in the experiments was the in-house distilled water.

Protein Samples (References)

A recombinant human homodimer fusion glycoprotein obtained from cultured Chinese hamster ovary cells (CHO), consisting of the first extracellular domain of a human protein (later referred as the fused domain) fused to the hinge, C_H2, and C_H3 sequences of a human immunoglobulin G_1 (IgG_1) was used as a model protein. The two polypeptide chains are linked in a dimeric structure by two disulfide bonds in the hinge region. The corresponding F_c fragment of the fusion protein (the hinge, C_H2, and C_H3 domains) was obtained by enzymatic cleavage. Both samples were dialyzed, using a Slide-A-Lyzer 10K cassette (Pierce, Rockford, IL), against 25 mM citrate, 2% w/v mannitol, and 1% w/v glycine at pH 7 and stored at 2–8°C until further testing.

Protein Samples (Pellet and Supernatant)

Visible aggregates of the fusion protein were observed after prolonged exposure (ca. 1 week) to siliconized glass. The protein solution contained 25 mg/mL fusion protein, 25 mM citrate, 2% w/v mannitol, and 1% w/v glycine at pH 7. The visible aggregates were separated from the soluble protein by centrifugation at 3200 rpm in a Sorvall RT 6000D swinging bucket centrifuge after pooling the contents of several prefilled syringes in 15-mL polypropylene tubes. The supernatant fraction was set aside in polypropylene tubes at 2–8°C until further testing. The pellet was rinsed several times with buffer (25 mM citrate, 2% w/v mannitol, and 1% w/v glycine at pH 7) to remove any soluble protein. The absence of soluble protein in the final rinse buffer was checked by UV absorbance at 280 nm. The pellet was then set aside at 2–8°C until further testing.

Differential Scanning Calorimetry (DSC)

DSC thermograms of the reference fusion protein and F_c fragment in 25 mM citrate, 2% w/v mannitol, and 1% w/v glycine at pH 7 were performed using a VP-DSC calorimeter (MicroCal, Inc., Northampton, MA). Scans were obtained from 10 to 100°C under 2 atmospheres of pressure at a scan rate of 1.5°C/min. The protein concentrations of all samples were approximately 0.5 mg/mL. Protein and buffer samples were degassed prior to loading the DSC cells. A buffer baseline was subtracted from the protein scan.

Intrinsic Fluorescence

Intrinsic fluorescence measurements on the supernatant and pellet fractions of the fusion protein in 25 mM citrate, 2% w/v mannitol, and 1% w/v glycine at pH 7 were performed at 25°C using a FluoroMax-2 fluorescence spectrophotometer (Jobin Yvon, Inc., Edison, NJ). The excitation wavelength was 280 nm (with a slit opening of 3 nm) and the emission spectra were recorded from 300 to 420 nm (with a slit opening of 3 nm). The protein concentration was about 10 μg/mL. At that concentration, no scattering

Regeneron Ex. 2073
Alvotech v. Regeneron
PGR2025-00085
Page 2 of 15
RGN-EYLEA-BIOSIM-00741166

interferences from the visible aggregates were observed. Raman peaks were removed by subtraction of the emission buffer spectra from the protein emission spectra using Grams AI version 7.01 (Thermo Electron Corporation, Woburn, MA).

Reducing and Nonreducing SDS–PAGE

Visible particulate suspension and soluble fraction of the fusion protein were analyzed by reducing and nonreducing SDS–PAGE gel. Supernatant and pellet fractions of the fusion protein were separately incubated with and without 7M guanidine hydrochloride, in the absence and presence of 2-mercaptoethanol (3% w/v). These various samples were also analyzed by SDS–PAGE. Protein samples were mixed with either reducing or nonreducing SDS buffer and boiled for 5 min. The protein samples as well as a protein marker (Invitrogen, Carlsbad, CA) were loaded onto a precasted 4%–20% Tris/glycine gel (Invitrogen). About 10 μg of protein were loaded on the gel. The gel was stained with colloidal blue (Invitrogen) and distained in water.

ANS Fluorescence

Extrinsic fluorescence measurements were performed after mixing 8-anilino-1-naphtalene-sulfonate (ammonium salt), ANS, with either the supernatant or pellet fractions of the fusion protein. Both fractions were in 25 mM citrate, 2% w/v mannitol, and 1% w/v glycine at pH 7. Measurements were conducted at 25°C using a FluoroMax-2 fluorescence spectrophotometer (Jobin Yvon, Inc.). The exact concentration of the ANS stock solution in 25 mM citrate, 2% w/v mannitol, and 1% w/v glycine at pH 7 was determined by UV absorption at 350 nm of an ethanol dilution of the stock solution using a molar extinction coefficient of 5000/M · cm. The excitation wavelength was 380 nm (with a slit opening of 5 nm) and the emission spectra were recorded from 420 to 600 nm (with a slit opening of 5 nm). The protein and ANS concentrations were 0.06 and 5 μM, respectively.

Urea and Guanidine Hydrochloride Unfolding/Solubilization Equilibrium

The unfolding/solubilization of various protein samples in urea and guanidine hydrochloride was assessed by measuring the intrinsic fluorescence after incubation in increasing amounts of urea (from 0 to 8M) and guanidine hydrochloride (from 0 to 7M). The stock solutions of urea and guanidine hydrochloride were prepared in 25 mM citrate at pH 7, 2% w/v mannitol, 1% w/v glycine, in both the absence and presence of 2-mercaptoethanol (3% w/v). The pH of all stock solutions were subsequently readjusted to 7.0 with either concentrated HCl or NaOH solutions. The refractive index of the denaturant solutions and buffer were measured using a 60/ED refractometer equipped with a sodium lamp unit (Bellingham & Stanley, Inc., Lawrenceville, GA). The molarity of both stock solutions was calculated by using the difference in refractive index between the denaturant solution and corresponding buffer.[20] The change in fluorescence emission maximum position was used to assess protein unfolding. All samples were incubated for 12 h at room temperature to attain complete unfolding equilibrium. The protein concentration was about 5 μg/mL. Control experiments with protein concentration at 50 μg/mL were also performed to ensure that fluorescence signals obtained at 5 μg/mL were not significantly influenced by adsorbed protein on the cuvette wall. The fluorescence measurements were performed using a FluoroMax-2 fluorescence spectrophotometer (Jobin Yvon, Inc.) with an excitation wavelength of 280 nm (3 nm slit width) and recording the emission spectra from 300 to 420 nm (3 nm slit width). A two-state folding mechanism for each of the protein unfolding transitions was assumed. Sigmoidal curve-fits were subsequently used to determine the midpoints of the unfolding transitions (C_m). Measurements were performed in triplicate for the reference fusion protein and F_c fragment and the supernatant fraction of the fusion protein, and in duplicate for the pellet fraction of the fusion protein.

Urea and Guanidine Hydrochloride Refolding Equilibrium

The reversibility of unfolding of the supernatant and of unfolding/solubilization of the pellet fractions in urea and guanidine hydrochloride was assessed by measuring the intrinsic fluorescence of series of samples, prepared from protein stock solution previously unfolded in high concentration of denaturant (5 and 8M urea and 7M guanidine hydrochloride), containing decreasing amount of either chaotropic agents. The protein stock solutions were incubated for 12 h at room temperature before being diluted into aliquots

Regeneron Ex. 2073
Alvotech v. Regeneron
PGR2025-00085
Page 3 of 15
RGN-EYLEA-BIOSIM-00741167

with decreasing amounts of denaturants. These aliquots were further incubated for 12 h at room temperature samples before being analyzed by intrinsic fluorescence. The fluorescence measurements were performed using a FluoroMax-2 fluorescence spectrophotometer (Jobin Yvon, Inc.) with an excitation wavelength of 280 nm (3 nm slit width) and recording the emission spectra from 300 to 420 nm (3 nm slit width). The protein concentration was approximately 5 μg/mL. A two-state folding mechanism for each of the protein folding transitions was assumed. Sigmoidal curve-fits were subsequently used to fit the refolding data. Measurements were performed in triplicate for the supernatant fraction of the fusion protein, and in duplicate for the pellet fraction of the fusion protein.

Size Exclusion Chromatography

The oligomerization state of the supernatant fraction of the fusion protein in 25 mM citrate, 2% w/v mannitol, and 1% w/v glycine at pH 7 was assessed by size exclusion chromatography. A HPLC Waters Alliance 2690 system, equipped with a Waters diode array detector 996, a TSK SWxi guard column (Tosoh Bioscience, Montgomeryville, PA), and a G3000SWXL TSK-Gel column (Tosoh Bioscience, Montgomeryville, PA) was used. The mobile phase was composed of 100 mM sodium phosphate and 200 mM NaCl at pH 7.2. The flow rate was 1.0 mL/min. Approximately 50 μg of protein were injected on the column.

RESULTS AND DISCUSSION

Preliminary Results (F_c Fragment Vs. Reference Fusion Protein)

Preliminary experiments, comparing the F_c fragment portion of the fusion protein with the reference fusion protein were performed in order to assign some experimental data (i.e., calorimetric peaks or unfolding transitions) to particular domains of the fusion protein. This preliminary work enabled a better interpretation of the data when supernatant and pellet fractions of the fusion protein were later compared.

Micro-DSC experiments on the reference fusion protein and F_c fragment were performed to assess the unfolding behavior of both proteins. The ultimate goal was the correlation of each unfolding transition of the fusion protein to its particular domains (fused, C_H2, or C_H3 domains). The unfolding pattern thermogram of the F_c fragment revealed the presence of two transitions at 71.8 ± 0.3 and 84.3 ± 0.3°C (Fig. 1). This result is in agreement with Tischenko et al.[21] who showed, also by DSC, that the two C_H2 domains melted as a single cooperative block at a lower temperature

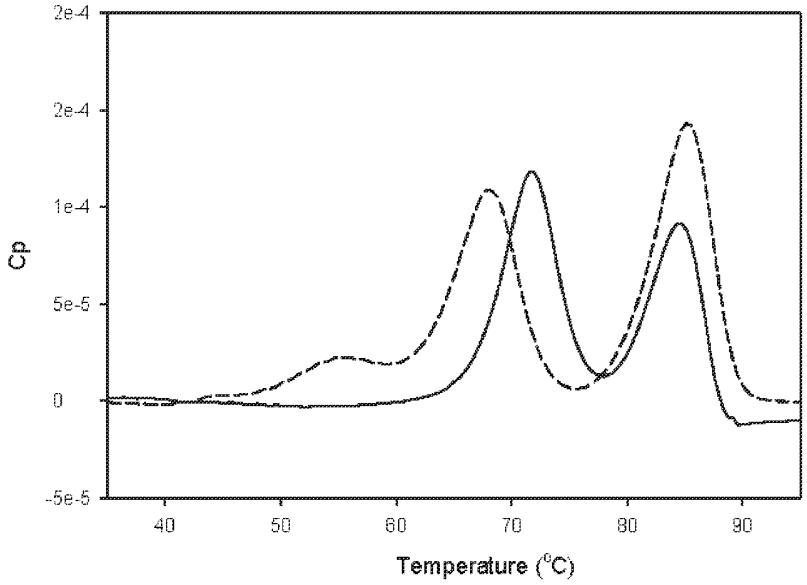


Figure 1. Representative differential scanning calorimetry (DSC) thermograms of the F_c fragment (solid line) and reference fusion protein (dashed line) in 25 mM citrate, 2% w/v mannitol, and 1% w/v glycine at pH 7.

Regeneron Ex. 2073
Alvotech v. Regeneron
PGR2025-00085
Page 4 of 15
RGN-EYLEA-BIOSIM-00741168

that the C_H3 domain block. Mimura et al.[22,23] also showed by deglycosylating the C_H2 domains of an IgG_1-Fc fragment that the C_H2 domains melted at a lower temperature than the C_H3 domain block. The thermogram of the fusion protein was characterized by three distinct unfolding transitions at 55.2 ± 0.05, 68.0 ± 0.1, and 85.2 ± 0.2°C (Fig. 1). The absence of a low-temperature unfolding transition in the F_c fragment thermogram indicates that the first unfolding transition of the fusion protein correspond to the fused domains. Therefore, based on the DSC experiments, it can be concluded that the three melting transitions observed with the fusion protein can be attributed to the fused, C_H2, and C_H3 domains, respectively. Interestingly, Figure 1 shows that the fused domains did not affect the stability of the C_H3 domains, whereas the significant difference in melting temperature of the C_H2 domains between the F_c fragment (71.8 ± 0.3°C) and the reference fusion protein (68.0 ± 0.1°C) could indicate a destabilization of the C_H2 domains by the fused domains.

In order to assess whether the order of unfolding of the three domains of the reference fusion protein observed by DSC experiments would parallel that observed by chaotropic agent-induced denaturation, urea (Fig. 2A) and guanidine hydrochloride (Fig. 2B) unfolding experiments on the reference fusion protein and F_c fragment were performed. The unfolding transitions were detected by changes in intrinsic fluorescence (maximum emission position) upon incubating both proteins in increasing amounts of urea or guanidine hydrochloride. Urea-induced unfolding revealed two unfolding transitions for the fusion protein, while only one unfolding transition was observed for the F_c fragment (Fig. 2A). The C_m values were 3.2 ± 0.03 and 6.1 ± 0.03M for the fusion protein and 6.3 ± 0.01M for the F_c fragment. Guanidine hydrochloride-induced unfolding of the reference fusion protein revealed three unfolding transitions at 0.8 ± 0.02, 2.2 ± 0.01, and 4.0 ± 0.30M, while only two transitions were detected at 2.1 ± 0.01, and 3.7 ± 0.06M for the F_c fragment (Fig. 2B). Although a significant amount of work has been done on the kinetics of unfolding and refolding of fragments of IgG_1,[24,25] a limited number of equilibrium experiments has been reported.[26] However, our data are in agreement with those from Sumi et al.,[26] who demonstrated that the C_H2 domains unfolded before the C_H3 domains in guanidine hydrochloride. Interestingly, urea, being a weaker chaotropic agent than guanidine hydrochloride, could most likely not promote the unfolding of the C_H3 domains for both the fusion protein and the F_c fragment. The fluorescence maximum emission values obtained for the fusion protein and the F_c fragment in the presence of 8M urea (352 and 350 nm, respectively) were similar to those measured in the plateau region between the second and third unfolding transitions in guanidine hydrochloride. This observation would indicate that in 8M urea, both the fusion protein and the F_c fragment were not fully unfolded (i.e., the C_H3 domains were most probably not unfolded). With both urea- and guanidine hydrochloride-unfolding

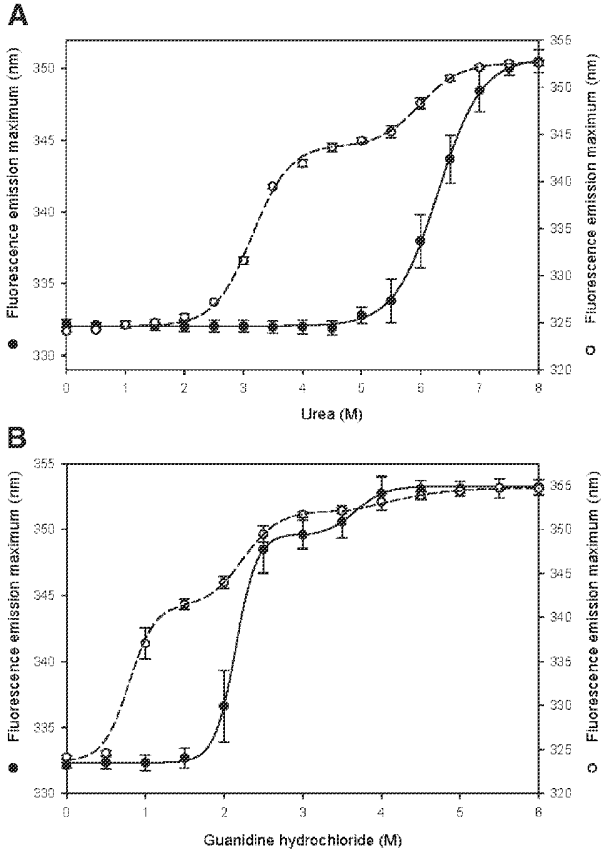


Figure 2. Unfolding of the F_c fragment (●) and fusion protein (○) in urea (A) and guanidine hydrochloride (B) in 25 mM citrate, 2% w/v mannitol, and 1% w/v glycine at pH 7. Maximum fluorescence emission was used to monitor the unfolding of both protein samples. The solid and dashed lines represent the best curve-fit for the determination of the urea (A) and guanidine hydrochloride (B) concentrations corresponding to the midpoint of the transitions (C_m) for the F_c fragment and fusion protein, respectively.

Regeneron Ex. 2073
Alvotech v. Regeneron
PGR2025-00085
Page 5 of 15
RGN-EYLEA-BIOSIM-00741169

experiments, the absence of the first unfolding transition in the F_c fragment sample indicates that the fused domains of the fusion protein unfold first, confirming the DSC experiments. As with heat denaturation, the three unfolding transitions observed with guanidine hydrochloride for the fusion protein can be attributed to the fused, C_H2, and C_H3 domains, respectively.

Visible Aggregates Versus Supernatant

After filtration of the visible aggregates no measurable decrease in protein concentration of the soluble fraction could be detected, indicating that the amount of visible aggregates was negligible, although pharmaceutically and clinically not acceptable. After separation by centrifugation, the visible particulates of the fusion protein (pellet) were compared to the supernatant by reducing and nonreducing SDS–PAGE, intrinsic fluorescence, ANS binding, urea and guanidine hydrochloride unfolding and refolding with and without 2-mercaptoethanol.

The visible particulates were initially analyzed by reducing and nonreducing SDS–PAGE (Fig. 3). The nonreduced supernatant fraction was characterized by a main band at about 115 kDa associated with faint impurity bands. This observation confirmed the SEC results on the supernatant fraction in which no significant increase in soluble aggregates was measured (0.8%) as compared to the reference fusion protein (0.7%). The nonreduced pellet fraction was also characterized by a main band at about 115 kDa, corresponding to the soluble protein, indicating that boiling the pellet in SDS resulted in the solubilization of some of the initially insoluble protein. However, some amount of insoluble aggregate was still observed in the sample as indicated by the smearing effect and the presence of some proteinaceous material at the bottom of the sample well (i.e., material too large to even enter the gel). In addition, a band of soluble aggregate (~200 kDa) was also observed in the pellet fraction. The reduced supernatant fraction was characterized by a main band at about 55 kDa associated with faint impurity bands. The reduced pellet fraction was characterized by a main band at 55 kDa, corresponding to the reduced solubilized protein. Some proteinaceous material was still observed at the bottom of the sample well, indicating the presence of insoluble material. Interestingly, the band of soluble aggregate was less apparent (although still detectable) in the reduced sample, possibly indicating the presence in the pellet of some covalently linked aggregated species. However, it is also possible that reducing

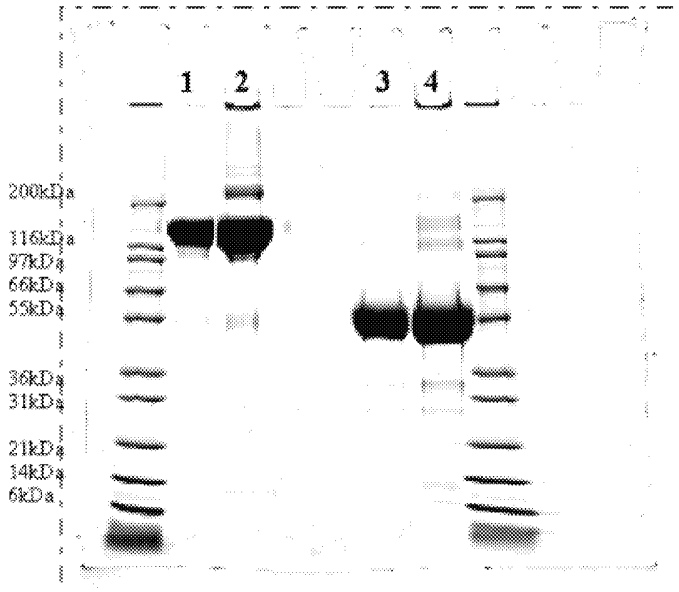


Figure 3. Reducing and nonreducing SDS–PAGE gel of supernatant and pellet fractions of the fusion protein. Lanes 1 and 2 represent the nonreduced supernatant and pellet fractions, respectively. Lanes 3 and 4 represent the reduced supernatant and pellet fractions, respectively.

Regeneron Ex. 2073
Alvotech v. Regeneron
PGR2025-00085
Page 6 of 15
RGN-EYLEA-BIOSIM-00741170

the samples enhanced the dissociation of noncovalently linked aggregates that could not have been dissociated in nonreducing conditions.

Significant differences in the fluorescence emission maximum were observed between the visible aggregates and the supernatant (Fig. 4). The fluorescence emission signal for the supernatant fraction following excitation at 280 nm (Fig. 4) was characterized by two maxima at 316 and 324 nm. A similar fluorescence emission profile was obtained following excitation at 295 nm (data not shown), indicating that the presence of these two maxima was most probably due to the presence of tryptophan residues in different states of solvation rather than a tyrosin influence on the fluorescence emission signal. A significant red shift from 316/324 nm for the supernatant to 332 nm for the particulates was detected, likely indicating a partial reorganization of the tertiary structure, thus resulting in the solvent exposure of one or several tryptophan residues.

Interestingly, a significant increase in ANS fluorescence intensity concomitant to a blue shift (from 522 to 508 nm) was observed for the particulates (Fig. 5), indicating the presence of partially folded structures in this sample.[27,28] On the other hand, no ANS binding was observed for the supernatant. This ANS binding experiment seemed to confirm the intrinsic fluorescence measurement; whereby the particulates appeared to be partially unfolded thus enabling binding of the extrinsic dye.

The unfolding behavior in urea of the supernatant and the unfolding/solubilization behavior of the pellet fractions of the fusion protein was compared by following fluorescence emission maximum (Fig. 6). For the pellet fraction, both solubilization and unfolding phenomena occur concomitantly in urea, complicating the interpretation of the data. The first transition, corresponding to the fused domains, was significantly different between the supernatant and the particulates (Fig. 6), although the corresponding C_m values did not significantly change (3.2 ± 0.03M for the supernatant and 3.4 ± 0.05M for the particulates). The smaller amplitude of change in the fluorescence emission maximum values observed for the pellet fraction likely reflected the partially unfolded state of the fused domains in the particulates previously detected by ANS binding and red-shifted intrinsic fluorescence. The similarity of the C_m values would indicate that the fused domains, although most probably partially unfolded, are not aggregated. The second transition, corresponding to the C_H2 domains, was not significantly different between the supernatant and the particulates (Fig. 6). Similar amplitude changes in the fluorescence emission maxima and C_m values (6.1 ± 0.03M for the supernatant and 6.3 ± 0.05M for the particulates) were

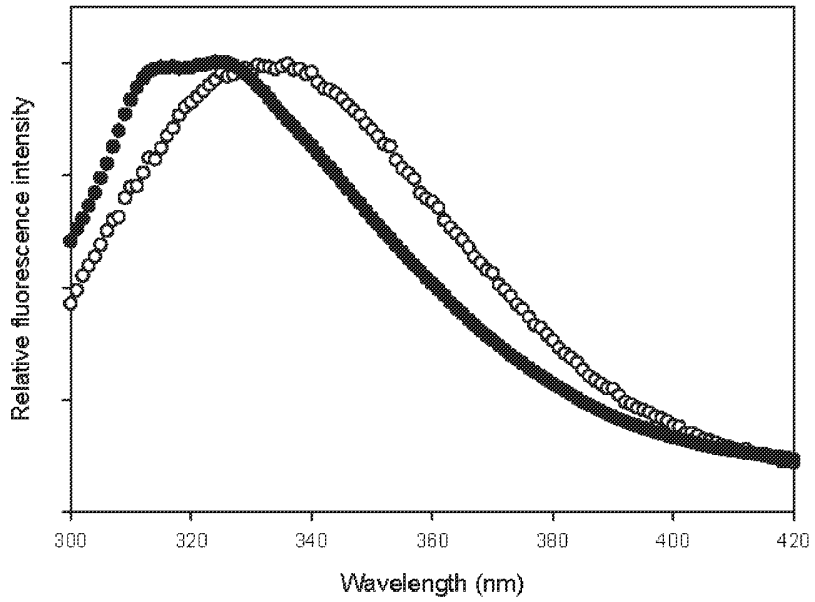


Figure 4. Intrinsic fluorescence emission spectra of the supernatant (●) and pellet (○) fractions of the fusion protein in 25 mM citrate, 2% w/v mannitol, and 1% w/v glycine at pH 7.

Regeneron Ex. 2073
Alvotech v. Regeneron
PGR2025-00085
Page 7 of 15
RGN-EYLEA-BIOSIM-00741171

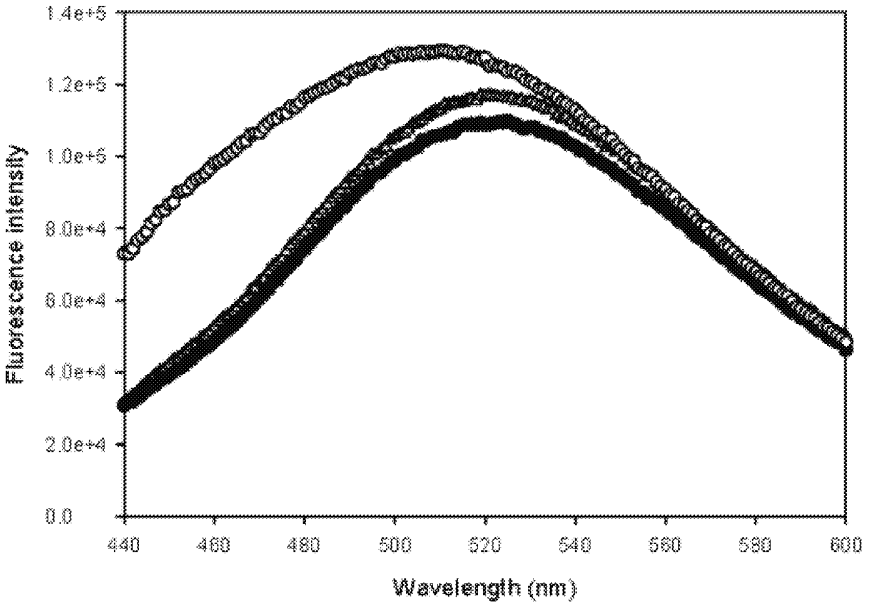


Figure 5. ANS fluorescence emission spectra when combined with the 25 mM citrate, 2% w/v mannitol, and 1% w/v glycine buffer at pH 7 (▲), the supernatant (●) and pellet (○) fractions of the fusion protein in 25 mM citrate, 2% w/v mannitol, and 1% w/v glycine at pH 7.

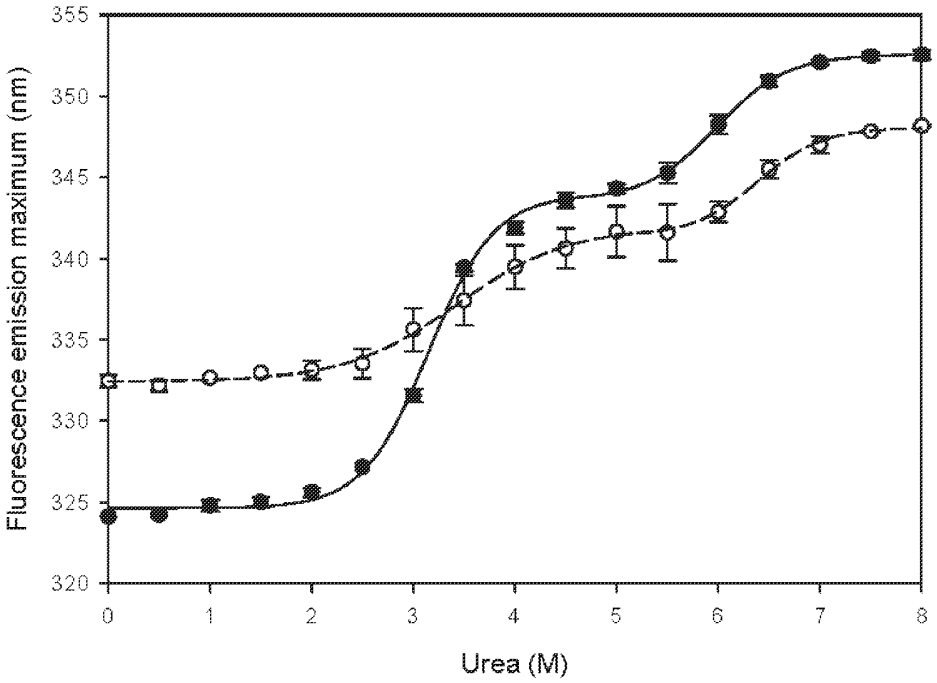


Figure 6. Unfolding of the supernatant (●) and pellet (○) fractions of the fusion protein in urea in 25 mM citrate, 2% w/v mannitol, and 1% w/v glycine at pH 7. Maximum fluorescence emission was used to monitor the unfolding of both protein samples. The solid and dashed lines represent the best curve-fit for the determination of the urea concentrations corresponding to the midpoint of the transitions (C_m) for the supernatant and pellet fractions, respectively.

Regeneron Ex. 2073
Alvotech v. Regeneron
PGR2025-00085
Page 8 of 15
RGN-EYLEA-BIOSIM-00741172

observed, most probably reflecting that the C_H2 domains are neither unfolded nor involved in the aggregation process. The fact that the fluorescence emission maximum values obtained for the particulates were still slightly blue shifted compared to those for the supernatant by 8M urea, seemed to indicate that aggregated species were still present in 8M urea, resulting in some tryptophan residues being buried.

The reversibility of unfolding of the supernatant and pellet fractions in urea was assessed after incubation both in 5 and 8M urea. After incubation in 5M urea, only the fused domains should have been unfolded in both fractions, while both the fused and C_H2 domains of both fractions should have been unfolded after incubation in 8M urea. After incubation in 5M urea, the unfolding of the supernatant fraction was completely reversible (Fig. 7A), the fluorescence emission maximum of the native fold (324 nm) being observed in the samples containing traces amounts of urea. The unfolding/solubilization of the pellet fraction after incubation in 5M urea was also reversible (Fig. 7A), the initial fluorescence emission maximum (332 nm) being observed for the samples containing trace amounts of urea. The reversibility of unfolding/solubilization of the pellet fraction indicates that the fused domains did not refold to their native conformation, but refolded to their initial partially folded/misfolded state, probably indicating that other domains of the protein, not affected by the incubation in 5M urea, were driving the misrefolding of the fused domains. Similar results were observed after incubation in 8M urea (Fig. 7B). Both sets of domains of the supernatant fraction refolded following the same profile as their unfolding, the native conformation being observed in the most urea-dilute sample (324 nm fluorescence emission maximum). Unfolding reversibility was also observed for the pellet fraction, both domains refolding via the same profile as their unfolding one (Fig. 7B). Again, the refolding of the particulates to their partially unfolded/misfolded state seems to indicate that other domains of the protein, not affected by the incubation in 8M urea, were driving the misrefolding of the fused domains.

The unfolding behavior in guanidine hydrochloride of the supernatant and the unfolding/solubilization behavior of the pellet fractions of the fusion protein were compared (Fig. 8A). The first transition (corresponding to the fused domains) was significantly different between the supernatant and the particulates. This guanidinium chloride data set confirmed the partial unfolding of the fused domains in the particulates (i.e., a smaller amplitude change in the fluorescence emission maximum values than for the supernatant fraction) and their lack of apparent involvement in the aggregation process (i.e., similar C_m value between the particulates, 0.7 ± 0.02M, and the soluble protein, 0.8 ± 0.02M). The second transition (C_H2 domains), similar to the urea unfolding experiment, seemed to indicate a native-like structure of the C_H2 domains in the particulates (similar amplitudes and C_m values for the particulates, 2.2 ± 0.05M, and the supernatant, 2.3 ± 0.02M). The third transition (C_H3 domains) was significantly different between the particulates and supernatant (Fig. 8a). A significant shift toward higher guanidinium chloride concentrations was observed for the C_m value of the particulates (5.2 ± 0.08M) as compared to that of the supernatant (4.1 ± 0.1M), most probably indicating the involvement of the C_H3 domains in the aggregation process. Although the fluorescence emission maximum values measured for the particulates at 7M guanidine hydrochloride were approaching those obtained for the supernatant at similar guanidine hydrochloride concentration, a significant difference in fluorescence emission maximum was still observed, most probably indicating that not all aggregates were dissociated in 7M guanidine hydrochloride. Boiling the pellet sample previously incubated in 7M guanidine hydrochloride did not result in any increase in fluorescence emission maximum as compared to that of the unboiled sample (data not shown), probably indicating extremely tight binding between some aggregates or the presence of covalently linked aggregates. The presence of insoluble materials in the pellet fraction incubated in 7 M guanidine hydrochloride was also confirmed by SDS–PAGE (Fig. 9). Despite the unavoidable poor quality of the gel due to the presence of high concentration of guanidine hydrochloride in some samples, the presence of insoluble protein could be clearly observed at the bottom of the well of the pellet fraction incubated in 7M guanidine hydrochloride (Fig. 9, lane 4).

The reversibility of unfolding in guanidine hydrochloride of the supernatant and pellet fractions was assessed after incubation in 8M guanidine hydrochloride. Post incubation, all three domains should have been theoretically unfolded in both fractions. Unfolding of the supernatant fraction was completely reversible (Fig. 8B), the fluorescence emission maximum of the native fold

Regeneron Ex. 2073
Alvotech v. Regeneron
PGR2025-00085
Page 9 of 15
RGN-EYLEA-BIOSIM-00741173

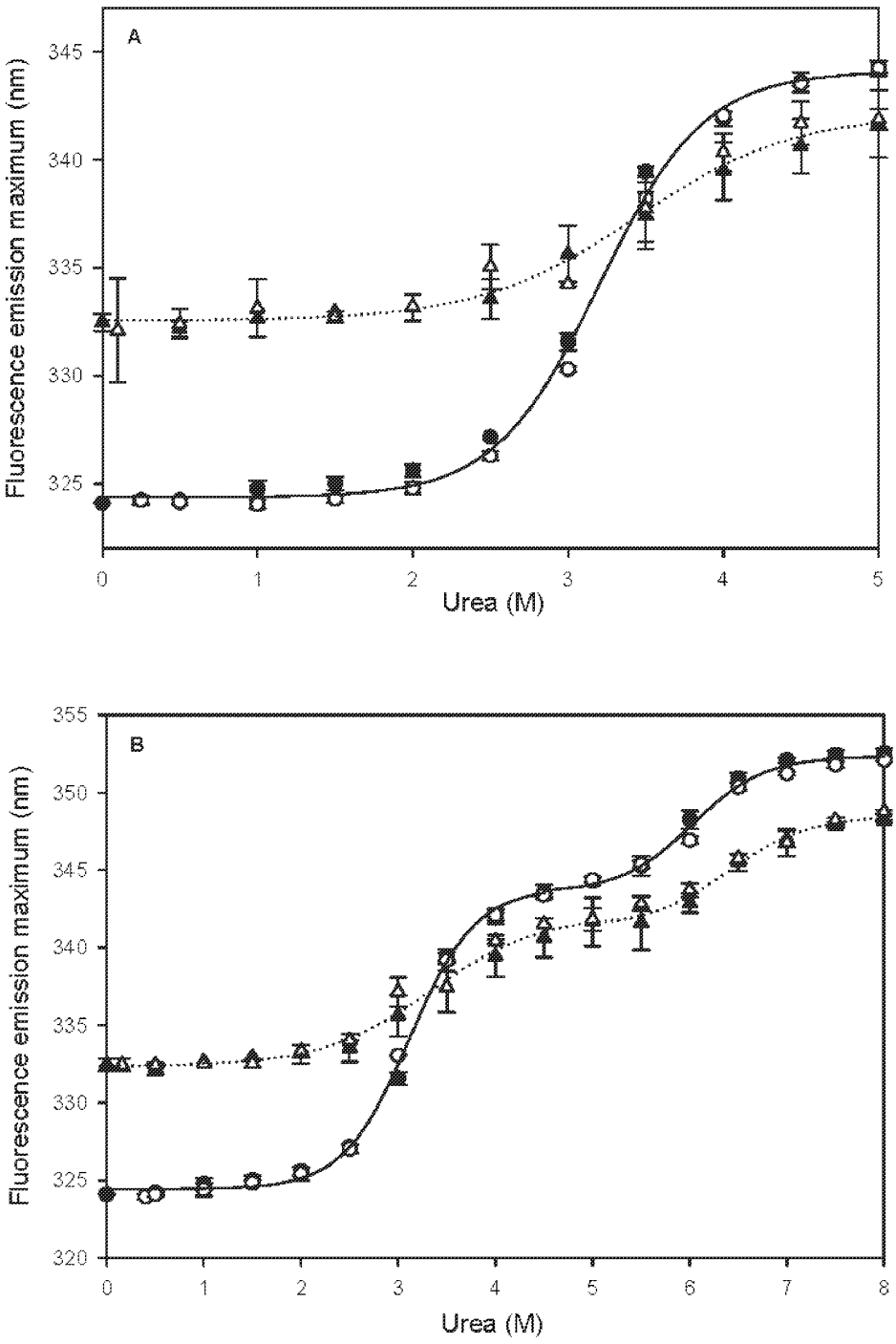


Figure 7. (A) Unfolding in urea (closed symbols) and refolding (open symbols) after incubation in 5M urea of the supernatant (circles) and pellet (triangles) fractions of the fusion protein in 25 mM citrate, 2% w/v mannitol, and 1% w/v glycine at pH 7. Maximum fluorescence emission was used to monitor the unfolding of both protein samples. The solid and dashed lines represent the best curve-fit for the combined (unfolding and refolding) data for the supernatant and pellet fractions, respectively. (B) Unfolding in urea (closed symbols) and refolding (open symbols) after incubation in 8M urea of the supernatant (circles) and pellet (triangles) fractions of the fusion protein in 25 mM citrate, 2% w/v mannitol, and 1% w/v glycine at pH 7. Maximum fluorescence emission was used to monitor the unfolding of both protein samples. The solid and dashed lines represent the best curve-fit for the combined (unfolding and refolding) data for the supernatant and pellet fractions, respectively.

Regeneron Ex. 2073
Alvotech v. Regeneron
PGR2025-00085
Page 10 of 15
RGN-EYLEA-BIOSIM-00741174

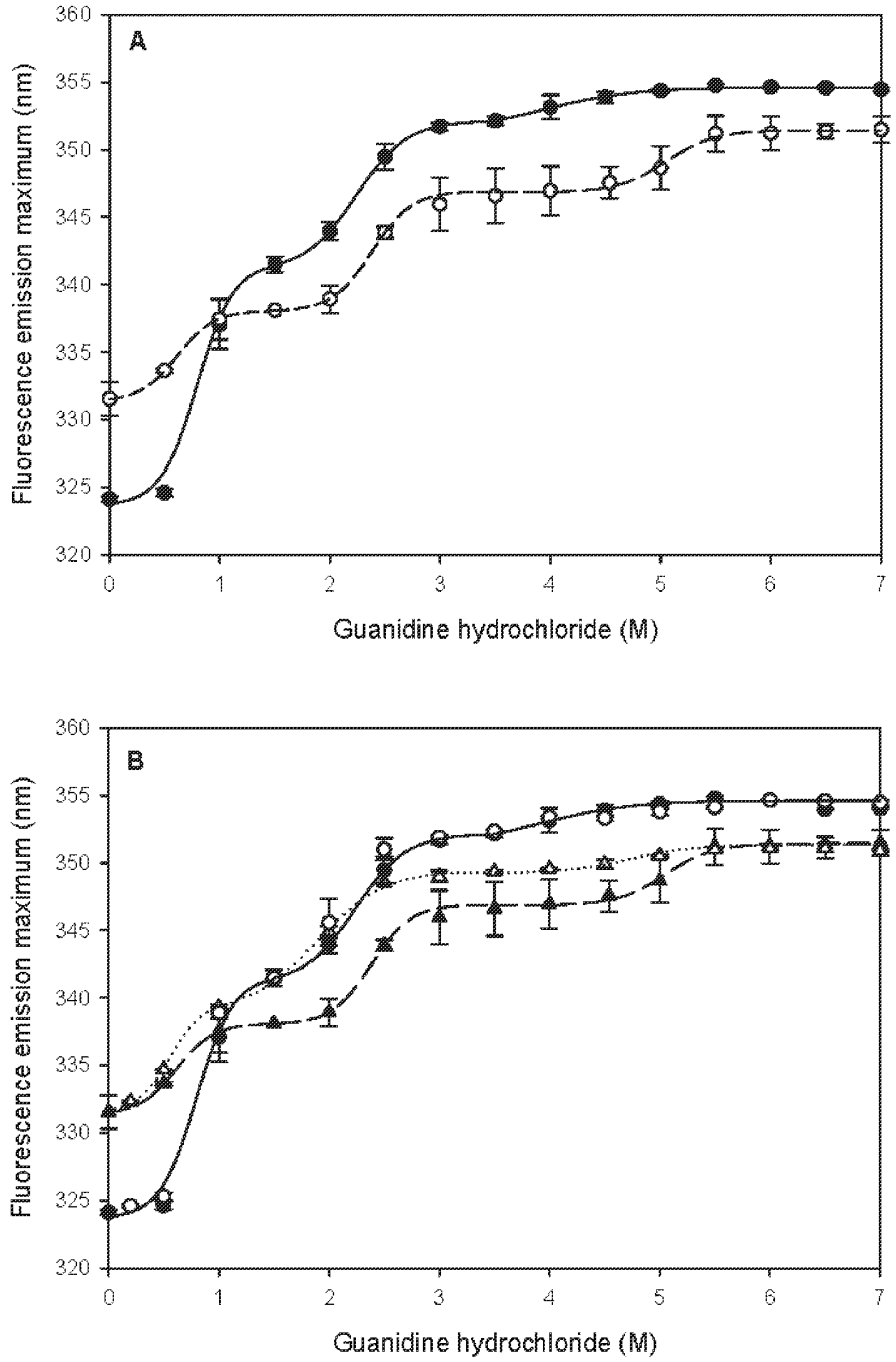


Figure 8. (A) Unfolding of the supernatant (●) and pellet (○) fractions of the fusion protein in guanidine hydrochloride in 25 mM citrate, 2% w/v mannitol, and 1% w/v glycine at pH 7. Maximum fluorescence emission was used to monitor the unfolding of both protein samples. The solid and dashed lines represent the best curve-fit for the determination of the guanidine hydrochloride concentrations corresponding to the midpoint of the transitions (C_m) for the supernatant and pellet, respectively. (B) Unfolding in guanidine hydrochloride (closed symbols) and refolding (open symbols) after incubation in 8M guanidine hydrochloride of the supernatant (circles) and pellet (triangles) fractions of the fusion protein in 25 mM citrate, 2% w/v mannitol, and 1% w/v glycine at pH 7. Maximum fluorescence emission was used to monitor the unfolding of both protein samples. The solid line represent the best curve-fit for the combined (unfolding and refolding) data for the supernatant fraction. The dashed and dotted lines represent the best curve-fit for the pellet fraction data during unfolding and refolding, respectively.

Regeneron Ex. 2073
Alvotech v. Regeneron
PGR2025-00085
Page 11 of 15
RGN-EYLEA-BIOSIM-00741175

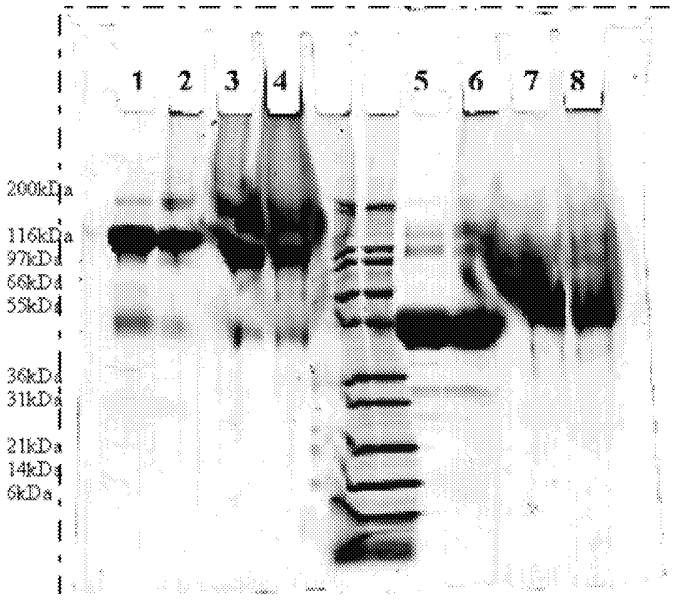


Figure 9. SDS–PAGE gel of supernatant and pellet fractions of the fusion protein incubated with and without 7M guanidine hydrochloride, in the absence and presence of 3% (w/v) 2-mercaptoethanol. Lanes 1–4 represent the nonreduced supernatant and pellet fractions incubated in the absence and presence of 7M guanidine hydrochloride, respectively. Lanes 5–8 represent the reduced supernatant and pellet fractions incubated in the absence and presence of 7M guanidine hydrochloride, respectively.

(324 nm) being observed in the samples containing traces amounts of guanidine hydrochloride. The unfolding of the pellet fraction induced by 8M guanidine hydrochloride appeared to be irreversible, as an obvious hysteresis was observed in the refolding experiment (Fig. 8B). The fluorescence emission values obtained during the refolding of the pellet fraction were in between those measured for the unfolding of the pellet fraction and the refolding of the supernatant fraction, probably indicating that the species present in the pellet fraction after incubation in 8M guanidine hydrochloride were a mixture of soluble and still aggregated species. This experiment seems to confirm the nonreducing SDS–PAGE gel in which the boiling in SDS resulted in the solubilization of some aggregated species, although aggregated material was still present. The same refolding experiment of the pellet fraction was repeated after the incubated sample in 8M guanidine hydrochloride was boiled for 5 min. Interestingly, no difference in the refolding pattern between the boiled and unboiled samples was observed (data not shown), indicating that boiling did not result in further dissociation of the aggregates.

Similar folding and refolding experiments in guanidine hydrochloride were performed in the presence of 3% (w/v) 2-mercaptoethanol (Fig. 10). The unfolding of the supernatant fraction in reducing conditions resulted in only two unfolding transitions with C_m values of 1.1 ± 0.01 and 3.1 ± 0.07M. The unfolding was not completely reversible (only one transition being observed during the refolding), although the conformation of the refolded protein appeared to reach a similar conformation than that of the fusion protein prior to its unfolding in reducing conditions (at least as observed by fluorescence emission maximum position). The unfolding of the pellet fraction was also characterized by two unfolding transitions with C_m values of 1.1 ± 0.2 and 3.3 ± 0.02M. Interestingly, as observed in nonreducing conditions, the fluorescence emission maximum values obtained for the pellet fraction as compared to those for the supernatant fraction were red shifted by about 7 nm in the absence of guanidine hydrochloride, but were blue shifted by about 4 nm in the presence of 7M guanidine hydrochloride. The initial red shift, most probably indicate the partial unfolding of the fusion protein in the pellet fraction, while the blue shift seems to indicate that aggregates were still present at high guanidine hydrochloride concentration, despite the presence of 3% (w/v) 2-mercaptoethanol. This

Regeneron Ex. 2073
Alvotech v. Regeneron
PGR2025-00085
Page 12 of 15
RGN-EYLEA-BIOSIM-00741176

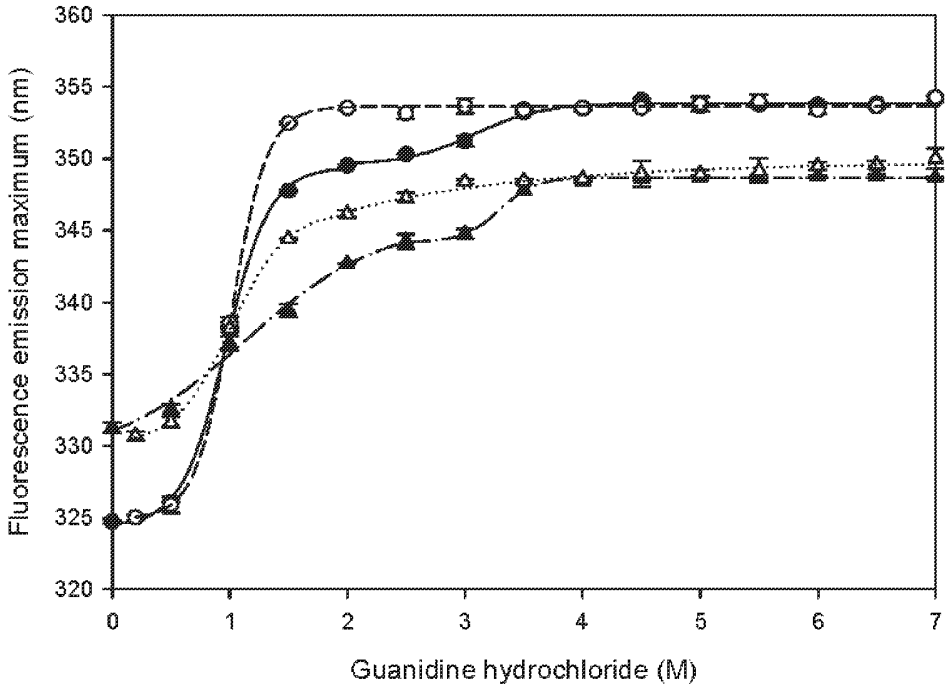


Figure 10. Unfolding in guanidine hydrochloride and 2-mercaptoethanol (closed symbols) and refolding (open symbols) after incubation in 8M guanidine hydrochloride and 2-mercaptoethanol of the supernatant (circles) and pellet (triangles) fractions of the fusion protein in 25 mM citrate, 2% w/v mannitol, and 1% w/v glycine at pH 7. Maximum fluorescence emission was used to monitor the unfolding and refolding of both protein samples. The solid and dashed lines represent the best curve-fit for supernatant fraction data during unfolding and refolding, respectively. The dash-dotted and dotted lines represent the best curve-fit for the pellet fraction data during unfolding and refolding, respectively.

observation proves that the putative presence of covalently linked aggregates in the pellet fraction is not the reason for the nonsolubilization of the aggregates in 7M guanidine (nonreducing condition). Instead, very strong noncovalent binding between protein molecules seems to preclude the aggregates from complete dissociation in high guanidine hydrochloride (Fig. 8A) or boiling SDS buffer (Fig. 3). However, the presence of nonreducible covalently-linked aggregates (i.e., ditorysine) could also be a potential explanation for these results. The presence of insoluble aggregates after incubation of the pellet fraction in 8M guanidine hydrochloride and 3% (w/v) 2-mercaptoethanol was confirmed by SDS–PAGE (Fig. 9, lane 8), a proteinaceous deposition at the bottom of the well being clearly observed. As expected, the unfolding of the aggregated species was not completely reversible and fluorescence emission values obtained during the refolding of the pellet fraction were in between those measured for the unfolding of the pellet fraction and the refolding of the supernatant fraction (Fig. 10).

The formation of insoluble aggregates is usually regarded as a thermodynamically irreversible process; therefore, it is assumed that the growth phase should continue until no more soluble material is available. However, in this particular case, the aggregation process did not seem to grow exponentially but rather stops after only an insignificant amount of soluble protein has precipitated. In fact, the overall concentration of soluble protein was not measurably decreased by particulate formation. This phenomenon could possibly be explained by the preferential precipitation of only a subpopulation of the soluble protein. Another plausible explanation for such a phenomenon, would be the total consumption of a necessary putative cofactor (initially present at low levels).

Regeneron Ex. 2073
Alvotech v. Regeneron
PGR2025-00085
Page 13 of 15
RGN-EYLEA-BIOSIM-00741177

CONCLUSIONS

The visible aggregates were characterized using several biophysical techniques. Despite the complexity of the protein structure, it was possible to pinpoint the differences between the visible aggregates and the soluble protein at the domain level. Based on these experiments it was possible to extrapolate that, in the pellet fraction (i) the extracellular domain of the protein was unfolded but not involved in the aggregation process, (ii) the C_H2 domain was native-like, and (iii) the C_H3 domain was involved in the aggregation process. Careful characterization of the aggregates should permit a more scientific rationale to solve aggregation issues whenever encountered.

ACKNOWLEDGMENTS

The author would like to thank Dr. Fred Taylor for supplying the F_c fragment and Mr. Angelo Polito for performing the SEC experiments.

REFERENCES

1. Fink AL. 1998. Protein aggregation: Folding aggregates, inclusion bodies and amyloid. Fold Des 3: 9–23.
2. Harper JD, Wong SS, Lieber CM, Lansbury PT, Jr. 1999. Assembly of A beta amyloid protofibrils: An *in vitro* model for a possible early event in Alzheimer's disease. Biochemistry 38:8972–8980.
3. Baskakov IV, Legname G, Baldwin MA, Prusiner SB, Cohen FE. 2002. Pathway complexity of prion protein assembly into amyloid. J Biol Chem 277: 21140–21148.
4. Buxbaum J. 1992. Mechanisms of disease: Monoclonal immunoglobulin deposition. Amyloidosis, light chain deposition disease, and light and heavy chain deposition disease. Hematol Oncol Clin North Am 6:323–346.
5. Chi EY, Krishnan S, Randolph TW, Carpenter JF. 2003. Physical stability of proteins in aqueous solution: Mechanism and driving forces in nonnative protein aggregation. Pharm Res 20:1325–1336.
6. Grillo AO, Edwards KL, Kashi RS, Shipley KM, Hu L, Besman MJ, Middaugh CR. 2001. Conformational origin of the aggregation of recombinant human factor VIII. Biochemistry 40:586–595.
7. Treuheit MJ, Kosky AA, Brems DN. 2002. Inverse relationship of protein concentration and aggregation. Pharm Res 19:511–516.
8. Walsh DM, Lomakin A, Benedek GB, Condron MM, Teplow DB. 1997. Amyloid beta-protein fibrillogenesis. Detection of a protofibrillar intermediate. J Biol Chem 272:22364–22372.
9. Kendrick BS, Cleland JL, Lam X, Nguyen T, Randolph TW, Manning MC, Carpenter JF. 1998. Aggregation of recombinant human interferon gamma: Kinetics and structural transitions. J Pharm Sci 87:1069–1076.
10. Khurana R, Gillespie JR, Talapatra A, Minert LJ, Ionescu-Zanetti C, Millett I, Fink AL. 2001. Partially folded intermediates as critical precursors of light chain amyloid fibrils and amorphous aggregates. Biochemistry 40:3525–3535.
11. Manning MC, Patel K, Borchardt RT. 1989. Stability of protein pharmaceuticals. Pharm Res 6:903–918.
12. Volkin DB, Mach H, Middaugh CR. 1997. Degradative covalent reactions important to protein stability. Mol Biotechnol 8:105–122.
13. Chen BL, Arakawa T, Morris CF, Kenney WC, Wells CM, Pitt CG. 1994. Aggregation pathway of recombinant human keratinocyte growth factor and its stabilization. Pharm Res 11:1581–1587.
14. Kendrick BS, Carpenter JF, Cleland JL, Randolph TW. 1998. A transient expansion of the native state precedes aggregation of recombinant human interferon-gamma. Proc Natl Acad Sci USA 95:14142–14146.
15. Chi EY, Krishnan S, Kendrick BS, Chang BS, Carpenter JF, Randolph TW. 2003. Roles of conformational stability and colloidal stability in the aggregation of recombinant human granulocyte colony-stimulating factor. Protein Sci 12:903–913.
16. Roberts CJ, Darrington RT, Whitley MB. 2003. Irreversible aggregation of recombinant bovine granulocyte-colony stimulating factor (bG-CSF) and implications for predicting protein shelf life. J Pharm Sci 92:1095–1111.
17. Uversky VN, Fink AL. 2004. Conformational constraints for amyloid fibrillation: The importance of being unfolded. Biochim Biophys Acta 1698:131–153.
18. Polverino de Laureto P, Taddei N, Frare E, Capanni C, Costantini S, Zurdo J, Chiti F, Dobson CM, Fontana A. 2003. Protein aggregation and amyloid fibril formation by an SH3 domain probed by limited proteolysis. J Mol Biol 334:129–141.
19. Uversky VN. 1999. A multiparametric approach to studies of self-organization of globular proteins. Biochemistry (Moscow) 64:250–266.
20. Pace CN, Scholtz JM. 1997. Measuring the conformational stability of a protein. In: Creighton TE, editor. Protein: A practical approach, 2nd edn. New York: Oxford University Press Inc, pp 299–321.
21. Tischenko VM, Vyacheslav M, Zav'yalov VP. 1998. Investigation of the cooperative structure of F_c fragments from myeloma immunoglobulin G. Biochemistry 37:5576–5581.

Regeneron Ex. 2073
Alvotech v. Regeneron
PGR2025-00085
Page 14 of 15
RGN-EYLEA-BIOSIM-00741178

22. Mimura Y, Church S, Ghirlando R, Ashton PR, Dong S, Goodall M, Lund J, Jefferis R. 2000. The influence of glycosylation on the thermal stability and effector function expression of human IgG1-Fc: Properties of a series of truncated glycoforms. Mol Immunol 37:697–706.
23. Mimura Y, Sondermann P, Ghirlando R, Lund J, Young SP, Goodall M, Jefferis R. 2001. Role of oligosaccharide residues of IgG1-Fc in Fc gamma RIIb binding. J Biol Chem 276:45539–45547.
24. Goto Y, Hamaguchi K. 1982. Unfolding and refolding of the constant fragment of the immunoglobulin light chain. J Mol Biol 156:891–910.
25. Goto Y, Hamaguchi K. 1982. Unfolding and refolding of the reduced constant fragment of the immunoglobulin light chain. Kinetic role of the intrachain disulfide bond. J Mol Biol 156:911–926.
26. Sumi A, Hamaguchi K. 1982. Denaturation by guanidine hydrochloride of the Fc(t) and pFc' fragments of human immunoglobulin G. J Biochem 92:823–833.
27. Stryer L. 1968. Fluorescence spectroscopy of proteins: Fluorescent probes provide insight into the structure, interactions, and dynamics of proteins. Science 162:526–533.
28. Semisotnov GV, Rodionova NA, Razgulyaev OI, Uversky VN, Gripas AF, Gilmanshin RI. 1991. Study of the "molten globule" intermediate state in protein folding by a hydrophobic fluorescent probe. Biopolymers 31:119–128.

Regeneron Ex. 2073
Alvotech v. Regeneron
PGR2025-00085
Page 15 of 15
RGN-EYLEA-BIOSIM-00741179